Journal of Plant Protection Research

eISSN 1899-007X

ORIGINAL ARTICLE

A comparative study of the antifungal activity of silver nanoparticles prepared from *Moringa oleifera* and *Spirulina platensis* extracts against *Aspergillus parasiticus* isolated from Egyptian wheat grains

Zakaria Awad Baka*®

Botany and Microbiology, Faculty of Science, University of Damietta, New Damietta, Egypt

Vol. 65, No. 3: 324-338, 2025

DOI: 10.24425/jppr.2025.155784

Received: June 15, 2024 Accepted: August 20, 2024 Online publication: September 17, 2025

*Corresponding address: zakariabaka@yahoo.com

Responsible Editor: Piotr Iwaniuk

Abstract

This work aimed to investigate the *in vitro* antifungal capability of silver nanoparticles (AgNPs) that were biosynthesized from extracts of two bioagents (*Moringa oleifera* and *Spirulina platensis*) against *Aspergillus parasiticus* attained from Egyptian wheat grains. *A. parasiticus* exhibited the most established species, additionally, the metabolite of isolate 3 generated a better quantity of Aflatoxin B1 (899.8 $\mu g \cdot l^{-1}$). AgNPs prepared from bioagent extracts inhibited the fungal mycelia and spore germination, even though *S. platensis* extract was more potent. The extract of *S. platensis* confirmed 22 phenolic compounds, with epicatechin (3455.9 $\mu g \cdot g^{-1}$ DW) recording the largest quantity. In evaluation, *M. oleifera* leaf extract revealed the existence of 16 phenolic compounds, with chlorogenic acid verifying the very best degree (3250.9 $\mu g \cdot g^{-1}$ DW). Fungal mycelia treated with 10% AgNPs showed intense deformation in comparison to the control, as found through scanning and transmission electron microscopy.

Keywords: AgNPs, Aspergillus parasiticus, Moringa oleifera, Spirulina platensis

Introduction

Wheat (*Triticum aestivum* L.) plays a crucial role in Egypt and other Mediterranean countries as an essential annual grain crop and a significant component of crop rotation. Throughout history, wheat has been a fundamental source of sustenance for humanity (Igrejas and Branlard 2020). It is recognized globally as a major agricultural commodity and a vital dietary staple with exceptional nutritional value (Guzmán *et al.* 2022). In Egypt, wheat holds the position of a primary strategic food crop (Khalil *et al.* 2020), contributing over one-third of the daily caloric intake and 45% of the total daily protein consumption for Egyptian consumers (Abdalla *et al.* 2023).

Fungal contamination of wheat grains poses a significant global concern for both human and animal health. These molds have the ability to produce mycotoxins, which are toxic substances. Toxigenic fungi

under specific conditions of humidity, temperature, and oxygen pressure produce mycotoxins (Schmidt *et al.* 2016). Amongst the various mycotoxins, aflatoxins are commonly reported in clinical toxicities. These carcinogens have been linked to a range of diseases, including cancer (Kimanya *et al.* 2021). Scientific literature indicates that aflatoxins have teratogenic, mutagenic, and carcinogenic properties. Consequently, their presence in the human food chain poses a significant public health risk. Several species of *Aspergillus*, such as *A. parasiticus*, *A. flavus*, and *A. nomius*, are known to be aflatoxin-producing fungi that can be found on various types of wheat (Shabeer *et al.* 2022).

Various antifungal agents, including extracts of plants and microalgae, can effectively control aflatoxigenic fungi. Plant extracts have significantly contributed to enhancing seed quality, improving the field

emergence of plant seeds, and suppressing seed-borne diseases. Several researchers have documented the safe and successful application of plant extracts in the suppression of seed-borne fungi (Shishido *et al.* 2015; Al-Ghanayem 2017; de Almeida *et al.* 2021; Schoss *et al.* 2022; Ilyas and Manohara 2023).

Numerous studies have shown that the extract of *M. oleifera* leaf is a biopesticide that is environmentally friendly, cost-effective, and readily available. It has minimal ecological impact, and is effective in managing plant infections (Yadav *et al.* 2023). *Moringa oleifera* exhibits properties against phytopathogens responsible for causing major plant diseases (Patil *et al.* 2022). The application of *Moringa* leaf extract has led to notable improvements in disease and pest resistance, resulting in yield increases ranging from 20 to 35% (Dhakad *et al.* 2019).

Shishido et al. (2015) have reported that cyanobacteria can produce a wide range of antifungal compounds, including peptides, polyketides, and alkaloids. Among these organisms, the blue-green freshwater alga Spirulina platensis stands out as the first singlecelled organism capable of converting large amounts of carbon dioxide in the atmosphere into oxygen, thus supporting life on Earth. Spirulina is gaining recognition as the "food of the future" due to its remarkable ability to produce highly concentrated and nutritious food more efficiently than other types of algae (Jain 2023). Jain (2023) reported that Spirulina contains 65-71% complete protein, containing all the essential amino acids in correct proportions. Furthermore, Spirulina species also contain phenolic compounds such as caffeic, chlorogenic, salicylic, synaptic, and trans-cinnamic acids, which possess antifungal properties (Pagnussatt et al. 2016).

Phenolic compounds derived from plants, such as phenolic acids, flavonoids, stilbenes, and tannins, can hinder the growth and activity of numerous microorganisms. This includes pathogens associated with food as well as clinically significant bacteria, fungi, and protozoa (Lobiuc *et al.* 2023). Due to the diverse structures and chemical compositions of these molecules, they exhibit various antimicrobial effects. These effects can range from permeabilization and destabilization of the plasma membrane to the inhibition of extracellular enzymes (Górniak *et al.* 2019; Baka and El-Zahed 2023).

In recent years, there has been a focus on innovative methods to combat fungal diseases, such as the utilization of nanoparticles in drug development (Abdelaziz *et al.* 2021). Among these nanoparticles, silver nanoparticles (AgNPs) have been extensively studied and proven highly effective against pathogenic fungi (Hasanin *et al.* 2021; Salem *et al.* 2022). AgNPs exhibit various mechanisms of action, including interaction with plasma membranes, facilitating proton diffusion,

and ultimately causing cell death (Salleh *et al.* 2020). Additionally, they have the ability to bind to phosphate groups in DNA (Neves *et al.* 2021). AgNPs can also alter membrane permeability for protons and phosphate groups, interfere with sulfhydryl groups in proteins and enzymes, and disrupt the electron transport chain (Badmus *et al.* 2020).

The current investigation aimed to assess the impact of *M. oleifera* leaf and *S. platensis* extracts, as well as their biosynthesized silver nanoparticles on the growth and ultrastructure of *A. parasiticus*.

Materials and Methods

Isolation and morphological characterization of fungi

Wheat grains (Triticum aestivum L., Giza 171) were obtained from the Agricultural Research Center, Giza, Egypt. Fifty grains of wheat were surface sterilized using a 2.5% NaOCl solution for 1 min., followed by rinsing three times in sterile DW. The grain samples were then dried on sterile filter paper. Using sterile forceps, 50 grains were randomly chosen and placed in Petri dishes (10 grains per dish) with potato dextrose agar medium (PDA). The Petri dishes were incubated at 25°C for 6-10 days. A few days later, the dishes were inspected daily for fungal growth. The fungi from each colony were separated and transferred to sterilized PDA dishes. The color of the colony, the morphology of the hyphae, conidia, and conidiophores, as well as the arrangement of the spores, were utilized for macroscopic and microscopic identification. The identification process was carried out using the identification keys of Nyongesa et al. (2015) for Aspergillus, Ismail et al. (2015) for Fusarium, Gao et al. (2021) for Alternaria and Bessey (2020) for other fungi. The frequencies and percentages of the total counts were determined using the following formulas: % TC = number of isolation times / total number of fungal isolates × 100%; F = number of times of isolation / number of samples \times 100.

Molecular identification of Aspergillus parasiticus

With the help of the DNA Isolation Kit (Agilent Technologies, Santa Clara, CA, USA), the entire genomic DNA of mycelia was extracted. Using the universal fungal primers ITS1 and ITS4, the rDNA-ITS region was amplified (Rahimi *et al.* 2016). To run PCR, a thermal cycler with the appropriate cycling parameters was utilized. Purified PCR products were purified using QIA Quick PCR Purification Kit (Qiagen,



Chadstone, Australia) silica-membrane-based columns in accordance with the manufacturer's instructions. Following purification, the Agilent Bioanalyzer 2100 with LabChip DNA1000 (Agilent Technologies, CA, USA) was used to quantify the DNA fragments. Purified rDNAs amplified by A β aFor/Bt2b were identified and sequenced in the NCBI database using BLAST algorithms.

Aflatoxin extraction

Aflatoxins were extracted using the procedure described by Trombete *et al.* (2014). The samples were combined with the solvent (an equal amount of chloroform and methanol), shaken, filtered, 90% methanol was added in a separating funnel, the methanol layer was collected, allowed to evaporate in the water bath, washed with chloroform, and allowed to evaporate before transferring the sample to an HPLC test.

Aflatoxin standards

The concentration of each aflatoxin was determined using a UV spectrophotometer after creating standard solutions for each. These standards were then utilized to create mixed working standards for HPLC analysis.

Quantification of aflatoxins by HPLC

Aflatoxin extraction, purification, and quantification were performed by the HPLC technique in accordance with Trombete *et al.* (2014). The detector was tuned at ex = 365 nm, Em = 425 nm. Toluene, ethyl acetate, formic acid, and methanol (90:6:2:2, v/v) made up the mobile phase. The flow rate was 1.5 ml per min. Using several standard solutions made from methanol, calibration curves for each aflatoxin were found. Linear calibration graphs were created by graphing the peak area against the aflatoxin amount injected. By comparing the peak regions with the calibration curve, aflatoxins were quantified.

Antifungal agents

The herbarium in the Department of Botany and Microbiology at Damietta University in Egypt provided *M. oleifera* plants. *Spirulina platensis*, on the other hand, was isolated from a freshwater canal and identified according to the research conducted by Khan *et al.* (2022).

Preparation of *Moringa oleifera* leaf extract

Moringa oleifera leaves were sterilized with 0.1% HgCl₂, and washed with sterile DW multiple times. Following this, the leaves were air-dried at room temperature. The dried leaves were then finely ground into a powder

weighing 2.0 g, which was stored in polyethylene bags at 28°C. The powder was dissolved in 200 ml of methanol and left to stand at room temperature for 12 h. The resultant mixture was filtered using Whatman No. 1 filter paper. After evaporating the solvent, the dry extract was combined with dimethyl sulfoxide (DMSO), and adjusted to final concentrations of 2.5, 5.0, 7.0, and 10%.

Spirulina platensis growth requirements

In the study conducted by Soni *et al.* (2019), *S. platensis* was cultivated using a modified medium. To ensure optimal growth, each flask was subjected to agitation and aeration using an air pump, delivering 150 bubbles \cdot min⁻¹. through a sterilized plastic tube. The flasks were then placed in an incubator set at 30°C for 9 days. The pH level was maintained at 9.0, and the light intensity provided was 50 μ Em-2 \cdot s⁻¹.

Preparation of Spirulina platensis extract

The *S. platensis* extract was prepared by grinding 2.0 g of *S. platensis* materials into a fine powder, followed by multiple extractions in a Soxhlet extractor using 200 ml of methanol. After evaporating the solvent, the extract was filtered (Zanganeh *et al.* 2022) and stored in a refrigerator in airtight glass bottles until needed. To assess antifungal activity, the extract was mixed with DMSO and adjusted to final concentrations of 2.5, 5.0, 7.0, and 10%.

HPLC analysis of phenolic compounds

An HPLC system manufactured by Shimadzu Corp., Kyoto, Japan, which included an LC-10AD pump, SCL-10A system controller, and SPD-M10A photodiode array detector, was utilized for analysis of phenolic compounds. Phenolic acids were separated using a prepacked LiChrospher 100 RP-18 column (4250 mm, 5 μ m) from Merck in Darmstadt, Germany. The mobile phase, consisting of water, acetonitrile, and acetic acid (88:10:2; v/v/v), was introduced at a flow rate of 1 ml · min⁻¹. The detection of phenolic compounds was monitored at 320 nm.

Biosynthesis of silver nanoparticles (AgNPs)

The green synthesis of AgNPs was carried out by combining 3 ml of each extract with 40 ml of 1 mM aqueous ${\rm AgNO_3}$ solution in a test tube. The mixture was then incubated at 25°C for 5 h in the absence of light. As reported by Medda *et al.* (2015), the formation of AgNPs was confirmed by a color change of the colloidal solution from yellow to dark brown and from bright red to dark brown.

Characterization of silver nanoparticles

AgNPs were described by means of diverse methodologies. Initially, a color shift was seen using the USA-made ATi Unicam UV2 UV/VIS Spectrometer to identify the AgNPs. Wavelengths ranged from 370 to 750 nm. With the use of an FTIR spectrometer (Perkin-Elmer LS-55-Luminescence Spectrometer), the chemical conformation of the AgNPs was investigated. After being dried to powder at 75°C, the solutions from the powders were measured in the 4000-400 cm/ range using the KBr pellet method. A TEM JEOL JEM-2100 was used to investigate the AgNPs' morphology at a 200 kV speeding-up voltage. The surface charge of the NPs, the consistency of nano-colloidal solutions, and the size distribution by volume were all measured using the Zeta Potential Analyzer (Model Malvern Zeta-Size Nano-zs90, USA). A Shimadzu XRD 7000 was used to record the XRD spectrum and display the number of Bragg reflections indexed in line with the face-centered cubic (FCC) structure of metallic silver in X-ray diffraction (XRD) investigations.

Antifungal activity

Linear mycelial growth

Linear mycelial growth was measured in mm using a ruler, as stated by Hendricks et al. (2017). The study examined the antifungal potential of methanol extracts from M. oleifera leaves, S. platensis, and their biosynthesized AgNPs against A. parasiticus (specifically isolate AP3, known for its high aflatoxin B1 production). Prior to solidification of the media, different concentrations (2.5%, 5.0%, 7.0%, and 10%) of the extracts and biosynthesized AgNPs were added to the mixture in a 9-cm Petri dish. Fungal plugs with a diameter of 5 mm were then used to inoculate the Petri dishes. Mancozeb fungicide plates (containing 1 ml of 0.2% w/v) served as positive controls, while plates with sterile DW were used as negative controls. The Petri dishes were incubated for 11 days at 24°C in a growth chamber. The average diameter of three fungal colonies was utilized to determine the radial growth of the fungal mycelia.

Spore germination

A fungal culture aged 10 days was utilized to produce spore suspensions of *A. parasiticus* (isolate AP3) containing a minimum of 20–30 spores per microscopic field. On a hollow glass slide with a droplet (about 0.1 ml) of different extract concentrations and their biosynthesized AgNPs (2.5, 5.0, 7.0, and 10%), 0.1 ml of the spore suspension was introduced. These slides were placed in a humid chamber formed by folding filter paper twice and positioning it on the edges of Petri dishes.

The Petri dishes were subjected to a 24-h incubation period at 24°C. Three repetitions of each treatment were carried out. The following formula can be used to calculate the inhibition percentage of spore germination: Inhibition % of spore germination = No. of spores germinated / Total no. of spores examined \cdot 100%.

Ultrastructural studies

For this, transmission electron microscopy (TEM) and scanning electron microscopy (SEM) were used. For SEM, mycelial plugs were fixed in 3% glutaraldehyde in cacodylate buffer at pH 6.8, dehydrated in a graded acetone series, and then dried with a critical point dryer (Polaron CPD 7501, UK). Using a JFC-1600 autofine coater (Polaron SC7620, UK), the samples were coated with gold-palladium before being analyzed and captured on camera with a JEOL SEM (Model SEM-6400JSM-6360LV, JEOL Ltd., Japan). Regarding TEM, the fungal mycelia were pre-fixed in 3% glutaraldehyde in cacodylate buffer at pH 6.8, post-fixed in 1% OsO₄, dehydrated in a graded series of ethanol, and embedded in Spurr's resin. The ultrathin sections were cut using an ultramicrotome and stained with uranyl acetate followed by lead citrate prior to examination with a JEOL TEM (Model JEM-1230 TEM, JEOL Ltd., Japan).

Statistical analysis

SPSS version 18 was used to statistically analyze the data. The results were examined using an ANOVA test with a significance level of 0.05. To guarantee accuracy, the experiments were conducted three times. The data were described using the mean \pm standard error (SE). The intergroup interaction was evaluated using Duncan's multiple range test. Significant differences were defined as those with a P-value of less than 0.05.

Results

Morphological identification of fungi isolated from wheat grains

The data in Table 1 displays the percentages of total counts (TC%) and the frequencies of isolation (F%) for the fungal species identified from wheat grains. *Aspergillus* was the most prevalent and commonly found genus, accounting for 53.41% of the total count with an isolation frequency of 66%. *Fusarium* followed *Aspergillus* in dominance, representing 20.97% of the total count and a frequency of 26%. *Alternaria* ranked third with a total count of 11.29% and a frequency of 14%. *Penicillium* was fourth with a total count of 8.07% and a frequency of 10%. *Rhizopus* had the lowest total count of 6.45% and a frequency of 8%. Percentages



Table 1. Percentages and frequencies of fungal species isolated from 50 wheat grains

Fungal species	No. of isolates	%TC	% F
Alternaria	7	11.29	14
A. alternata	3	4.84	6
A. raphani	3	4.84	6
A. tenuissima	1	1.61	2
Aspergillus	33	53.41	66
A. parasiticus	10	16.13	20
A. flavus	7	11.30	14
A. fumigatus	6	9.86	12
A. niger	4	6.45	8
A. ochraceus	3	4.84	6
A. sydowii	3	3.23	4
Fusarium	13	20.97	26
F. graminearum	6	9.68	12
F. moniliforme	4	6.45	8
F. solani	3	4.84	6
Rhizopus stolonifer	4	6.45	8
Penicillium	5	8.07	10
P. digitatum	3	4.84	6
P. notatum	2	3.23	4
Total fungal isolates	62		

%TC – percentage of total count; % F – percentage of frequency

of total count and frequency were calculated according to the following: %TC – percentage of total count; % F – percentage of frequency.

Molecular identification of Aspergillus parasiticus isolates

Ten isolates of *A. parasiticus* were subjected to PCR amplification of the ITS region, resulting in a product size of approximately 705 bp. The band size observed in Figure 1 was consistent among all fungal isolates. To determine the identity of these isolates, a sequence similarity search was conducted using the nucleotide BLAST program at the National Center for Biotechnological Information (NCBI) in the U.S.A. As a result, all isolates were confirmed to be *A. parasiticus* (Table 2).

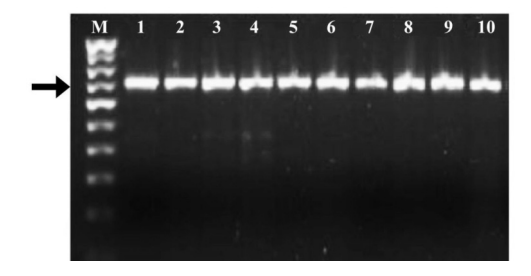


Fig. 1. Gel picture demonstrating a 705 bp (arrowhead) DNA fragment amplified in 10 *Aspergillus parasiticus* isolates on 1.2% agarose gel electrophoresis using ITS (1 and 4) primer

HPLC analysis of phenolic compounds

In the instance of *M. oleifera* leaf extract, 16 phenolic compounds were recovered. Chlorogenic acid recorded the highest quantity among all phenolic compounds (3250.9 $\mu g \cdot g^{-1}$ DW), followed by catechin (2321.5 $\mu g \cdot g^{-1}$ DW), and then caffeic acid (1091.7 $\mu g \cdot g^{-1}$ DW) (Table 3). Regarding *S. platensis*, 22 phenolic compounds were detected. Epicatechin displayed the highest concentration (3455.9 $\mu g \cdot g^{-1}$ DW), followed by catechin (2821.5 $\mu g \cdot g^{-1}$ DW), and then chlorogenic acid (920.9 $ug \cdot g^{-1}$ DW) (Table 4).

Aflatoxin production in culture media of Aspergillus parasiticus

Aspergillus parasiticus isolates were examined for aflatoxin production in culture media, and the data on toxigenic isolates can be found in Table 5. All isolates demonstrated toxicity with respect to AFB1 and AFB2. Isolate 3 recorded the highest levels of both toxins (899.8 and 142.5 $\mu g \cdot l^{-1}$, respectively), whereas isolate 9 showed the lowest levels of both toxins (82.1 and 33.1 $\mu g \cdot l^{-1}$, respectively).

Characterization of AgNPs

The characterization of AgNPs is represented in Figure 2, which shows the biosynthesis process from the extracts of *M. oleifera* leaves (Fig. 2A) and *S. platensis* (Fig. 2B). Upon the addition of AgNO₃, a color transformation was observed; the former changed from yellow to pink and the latter, from bright to dark brown.

Table 2. Molecular variability of *Aspergillus parasiticus* isolates

Groups	Isolate code	Accession number	Closest match	Similarity GenBank accessions	Frequency [%]
1	Ap1, Ap3, Ap9	NRRL3358	Clone 105	100	12.8
2	Ap2, Ap5, Ap7	NRRL3340	Clone 110	99.9	26.5
3	Ap4, Ap6	NRRL3356	Clone 116	100	14.7
4	Ap8, Ap10	NRRL3348	Clone 105	99.5	14.5

 Table 3. Phenolic compounds in Moringa oleifera leaves extract

Peak	Rt [min]	Compounds	Absorption spectra	Concentrations $[\mu g \cdot g^{-1} DW]$
1	1	gallic acid	288,241	320.2 ± 4.1
2	7.8	apigenin	301,276	76.8 ± 3.2
3	8.5	coumaric acid	356,212	125.9 ± 5.4
4	10.4	caffeic acid	325,278	1091.7 ± 10.3
5	12.8	catechin	420,263	2321.5 ± 8.4
6	14.6	chlorogenic acid	435,265	3250.9 ± 19.3
7	16.3	cinnamic acid	348,258	290.7 ± 6.4
8	20.8	kaermphereol	301,270	42.6 ± 2.3
9	22.5	ferulic acid	354,242	52.6 ± 3.1
10	24.9	qurecetin	420,245	530.5 ± 6.7
11	27.4	fumaric acid	322,265	25.9 ± 2.1
12	28.2	pinoresinol	421,280	158.9 ± 5.7
13	29.6	syrinigic acid	425,266	120.5 ± 4.7
14	30.5	myricetin	371,252	69.9 ± 6.7
15	32.7	vanillic acid	318,212	$9.8.6 \pm 1.8$
16	33.1	rutin	354,232	134.5 ± 8.6

 $[\]pm$ – standard error of the mean (n = 3)

Table 4. Phenolic compounds in *S. platensis* extract

Peak	Rt [min]	Compounds	Absorption	Concentrations $[\mu g \cdot g^{-1} DW]$
[min]	•	spectra		
1	1	cinnamic acid	288,241	310.2 ± 3.1
2	6.8	benzoic acid	301,276	86.7 ± 3.1
3	8.5	caffeic acid	356,212	124.9 ± 6.1
4	10.4	euganol	325,278	781.7 ± 10.3
5	12.8	catechin	420,263	2821.5 ± 8.4
6	14.6	chlorogenic acid	435,265	920.9 ± 15.3
7	18.2	kaermphereol	348,258	292.7 ± 5.1
8	20.5	gallic acid	301,270	142.6 ± 2.3
9	24.9	coumaric acid	354,242	62.6 ± 3.1
10	27.4	epicatechin	420,245	3455.9 ± 19.3
11	29.6	salicylic acid	322,265	45.8 ± 2.1
12	30.5	ferulic acid	421,280	160.9 ± 5.4
13	32.7	galangin	425,266	125.5 ± 4.1
14	33.1	synaptic acid	371,252	72.9 ± 5.7
15	35.6	genstein	318,212	101.6 ± 2.6
16	36.2	qurecetin	354,232	128.5 ± 7.5
17	38.1	myricetin	420,126	29.4 ± 1.5
18	40.9	pinostrobin	352,220	45.7 ± 2.1
19	41.5	pyrocatechol	302,321	119.8 ± 3.2
20	44.8	syrinigic acid	453.204	97.8 ± 2.3
21	45.9	rutin	450,120	89.5 ± 2.1
22	48.8	vanillic acid	371,243	132.6 ± 4.2

 $[\]pm$ – standard error of the mean (n = 3)



Table 5. Production of aflatoxins from isolates of *Aspergillus parasiticus*

our districts				
Isolates	Production of a	Production of aflatoxins [$\mu g \cdot l^{-1}$]		
1	AFB1	AFB2		
2	652.5	78.2		
3	899.8	142.5		
4	369.7	101.2		
5	297.3	82.2		
6	224.3	122.5		
7	135.0	118.8		
8	108.9	72.6		
9	82.1	33.1		
10	91.6	78.2		

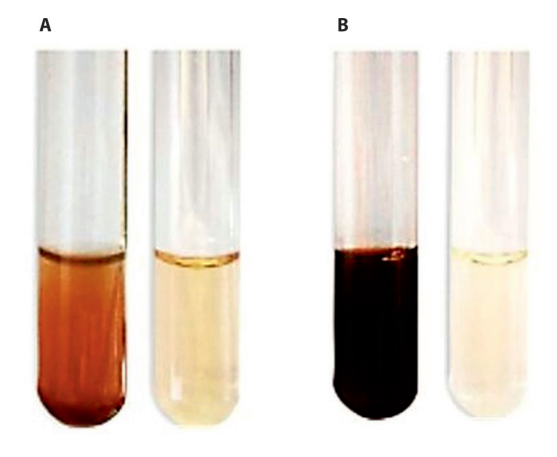


Fig. 2. Visual representation of biosynthesis of AgNPs. A – *Morgina oleifera* leaves extract; B – *Spirulina platensis* extract

Following a 72-h reaction period, the solution exhibited peak wavelengths of 412.94 nm and 423.50 nm on average for *M. oleifera* and *S. platensis*, respectively, as determined by UV-visible (UV-Vis) spectroscopy analysis (Fig. 3A, B).

FTIR measurements were conducted to elucidate the potential enhancement of bioreduction and stabilization of biosynthesized AgNPs using extracts from *M. oleifera* leaves and *S. platensis*. The FTIR spectra confirmed the reduction of mixtures in the extracts, with specific groups identified at distinct wavenumbers for each extract. For *M. oleifera* leaf extract, the groups were observed at 3419, 3913, 1642, 1745, and $1022 \cdot \text{cm}^{-1}$, while for *S. pratensis* extract, they were noted at 3432, 2925, 1656, 1359, and $1073 \cdot \text{cm}^{-1}$ (Fig. 4A, B).

Subsequent analysis of the optimized biosynthesized AgNPs using TEM revealed a size range of 10.0–16.69 nm for *M. oleifera* leaf extract and 9.45–17.15 nm for *S. pratensis* extract. The nanoparticles exhibited a uniform distribution and spherical shape (Fig. 5A, B).

Zetasizer analysis was employed to determine the zeta potential and size of the nanoparticle suspension. The average particle size of *M. oleifera* leaf extract was 20.60 nm, while *S. platensis* had a particle size of 14.20 nm. The zeta potential values indicated that the surface of AgNPs formed by *M. oleifera* leaf extract had a negative charge of approximately –16.8 mV, whereas the surface of AgNPs formed by *S. platensis* extract had a negative charge of around –19.4 mV (Fig. 6A, B).

To examine the crystalline characteristics of the biologically synthesized AgNPs, XRD analysis was conducted. The XRD pattern revealed the presence of four distinct diffraction peaks at two theta (2θ) angles of approximately 38° , 44° , 64° , and 78° , corresponding to the crystal planes 111, 200, 220, and 311, respectively (Fig. 7A, B).

Antifungal activity

Radial mycelial growth

Antifungal efficacy of crude extracts from *M. oleifera* leaves and *S. platensis*, as well as their synthesized AgNPs, were assessed *in vitro*. Both the crude extracts

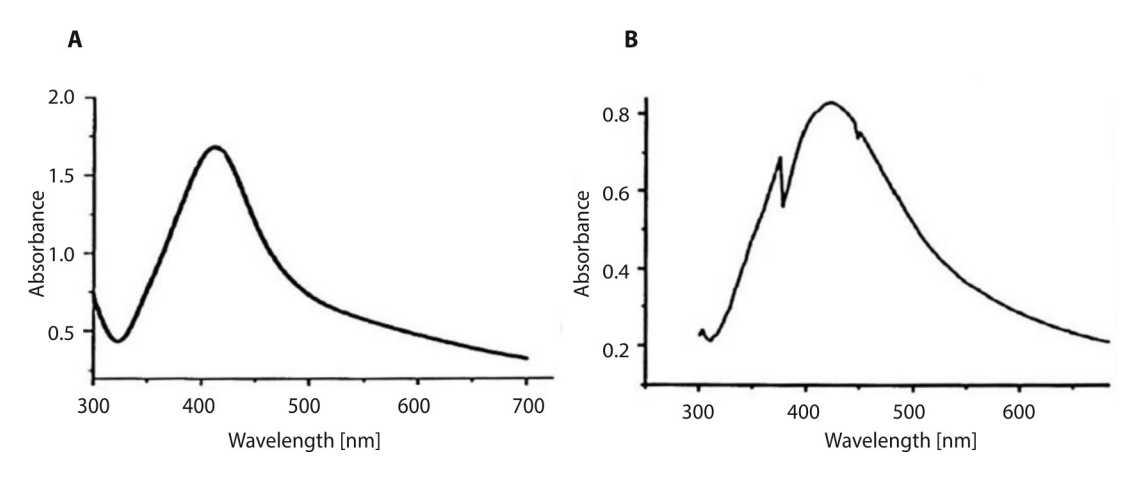
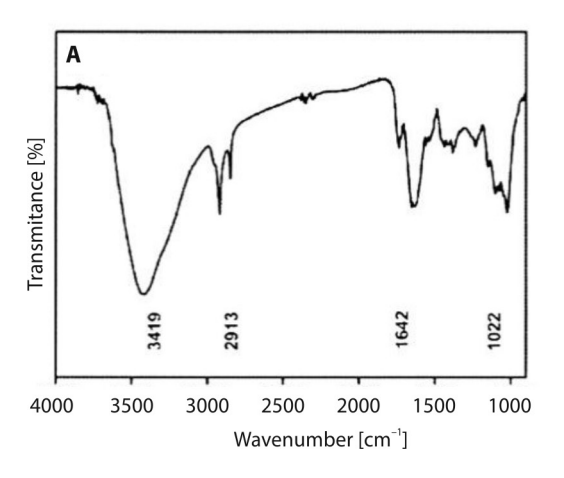


Fig. 3. The UV-Vis spectra reaction with AgNO, solution. A - Morgina oleifera leaf extract; B - Spirulina platensis extract



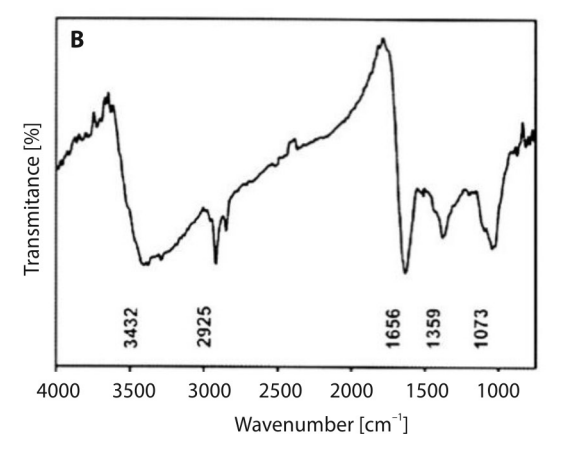


Fig. 4. FTIR adsorption spectra of AgNPs. A- prepared by Morgina oleifera leaf extract; prepared by Spirulina platensis extract

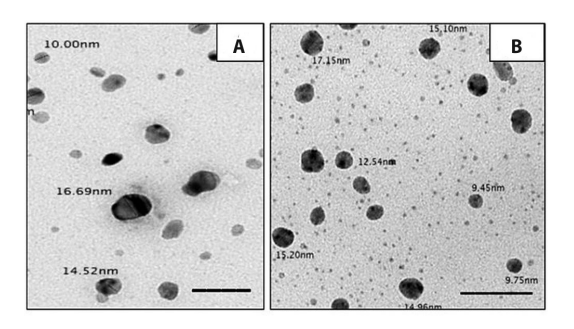
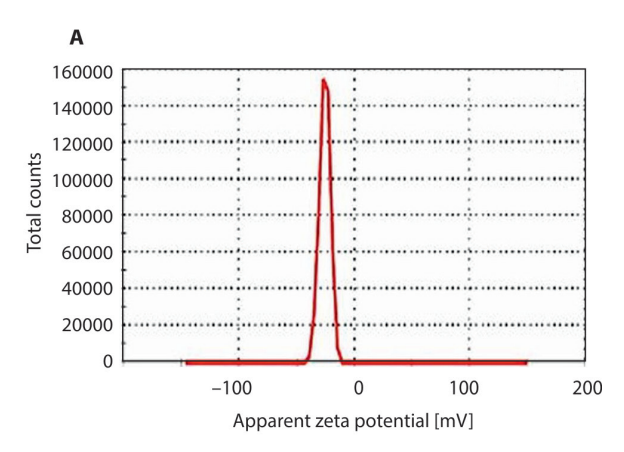


Fig. 5. TEM micrographs of biosynthesized AgNPs, displaying the size distribution ranges and spherical form of the nanocolloids. A – *Morgina oleifera* leaf extract; B – *Spirulina platensis* extract. Bar = 100 nm

and AgNPs inhibited the growth of *A. parasiticus* mycelium at all concentrations used, with the 10% concentration proving to be the most effective for both treatments (Fig. 8). The different bioagents investigated varied in their ability to impede mycelial growth using crude extracts and AgNPs. The diameter of *A. parasiticus* mycelial growth was reduced, with AgNPs being more effective than crude extracts. Furthermore, *S. platensis* extract and AgNPs exhibited a greater reduction in the mycelial growth than *M. oleifera* leaf extract. This concentration (10%) resulted in a decrease



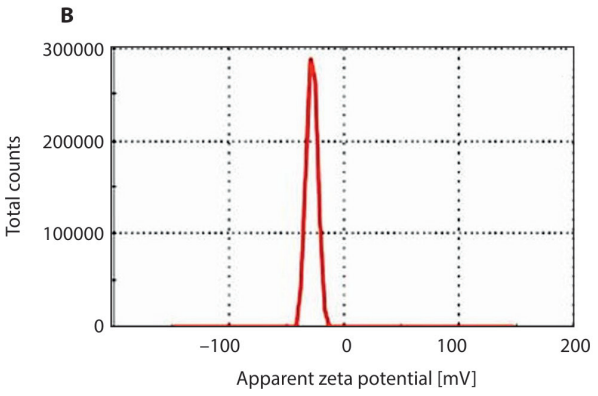
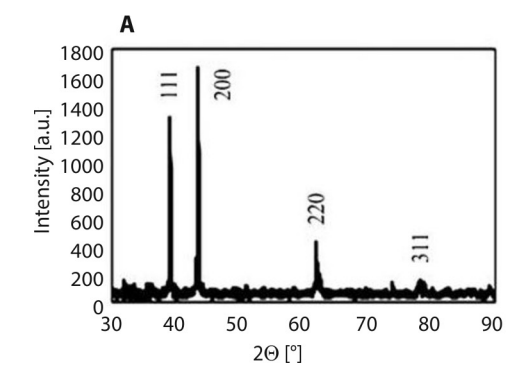


Fig. 6. Zeta potential of AgNPs synthesis. A – *Morgina oleifera* leaf extract (–16.8 mV); B – *Spirulina platensis* extract (–19.4 mV)



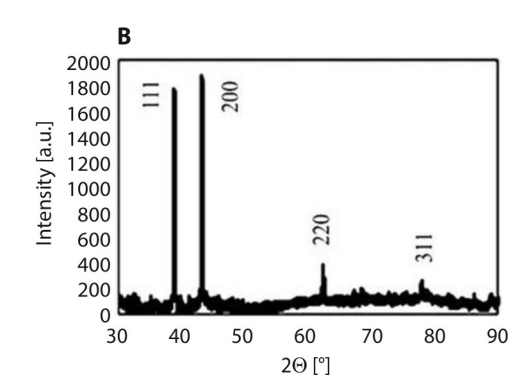


Fig. 7. XRD pattern. A – Morgina oleifera leaf extract; B – Spirulina platensis extract



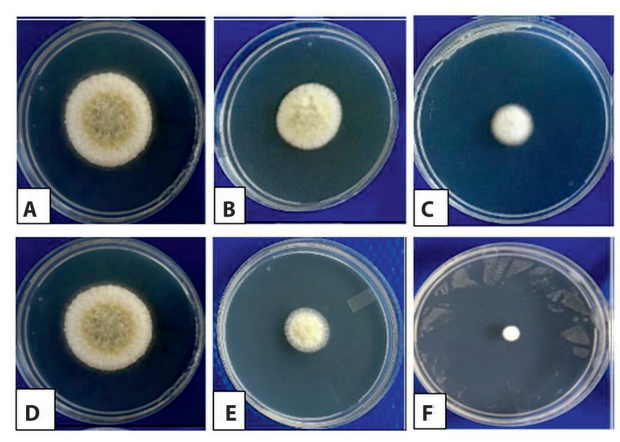


Fig. 8. Effect of crude extracts and AgNPs of *Morgina oleifera* and *Spirulina platensis* at 10% on radial mycelial growth of *Aspergillus parasiticus* (mm). A, D – control, medium only; B – crude extract of *M. oleifera* leaf; C – AgNPs of *M. oleifera* leaf extract; E – crude extract of *S. platensis* extract; F – AgNPs of *S. platensis* extract

in mycelial growth of the fungus when treated with *M. oleifera* leaf extract and AgNPs measuring 10.4 and 9.5 mm, respectively (Fig. 9A). Conversely, the same concentration led to a reduction in mycelial growth when treated with *S. platensis* extract, with AgNPs measuring 9.2 and 8.3 mm, respectively. The fungicide exhibited a reduction of 5.4 mm (Fig. 9B).

Spore germination

Spore germination was found to be significantly inhibited by the application of bioagent extracts and

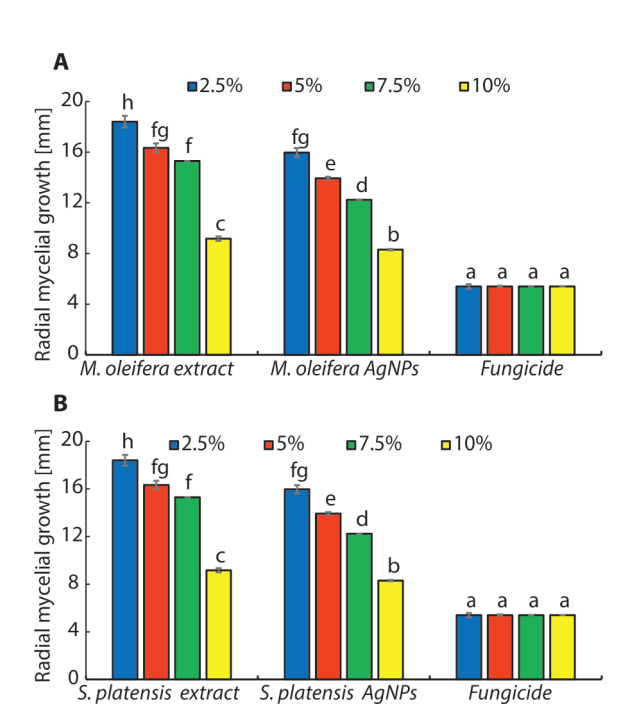


Fig. 9. Radial mycelial growth of *Aspergillus parasiticus* (mm); after treatment by crude extract, AgNPs, and fungicide at different concentrations. A – *Morgina oleifera*; B – *Spirulina platensis*. Duncan's multiple range test indicates that there is no significant difference between the lettered columns (p < 0.05, n = 3). The error bars show the SE of the mean

associated AgNPs, as indicated in Figure 10. Among the various doses tested, the highest concentration (10%) of crude extracts from *M. oleifera* leaves and *S. platensis*, along with their biosynthesized AgNPs, exhibited the greatest inhibition in the spore germination of *A. parasiticus*. Comparatively, AgNPs showed a higher percentage of spore germination inhibition than the crude extracts of the bioagents. The crude extract of *M. oleifera* leaves and AgNPs demonstrated inhibition in spore germination percentages of 70.6% and 73.5%, respectively. Similarly, the inhibition percentages for the *S. platensis* crude extract and AgNPs were 74.6% and 75.4%, respectively. In contrast, the fungicide exhibited a significant decrease in germination percentage of 85.4% (Fig. 10A, B).

Ultrastructural investigations

SEM observations

The effects of AgNPs biosynthesized from *M. oleifera* leaf and *S. platensis* extracts at a 10% concentration on the morphology of *A. parasiticus* were analyzed through SEM and are shown in Figure 11. The *A. parasiticus* mycelium grown on a PDA medium served as the control (Fig. 11A), exhibiting elongated, normal, uniform hyphae with a smooth outer surface. Upon the addition of AgNPs from *M. oleifera* extract to the medium, noticeable changes in hyphal morphology were observed, indicating twisted, flattened, and reduced

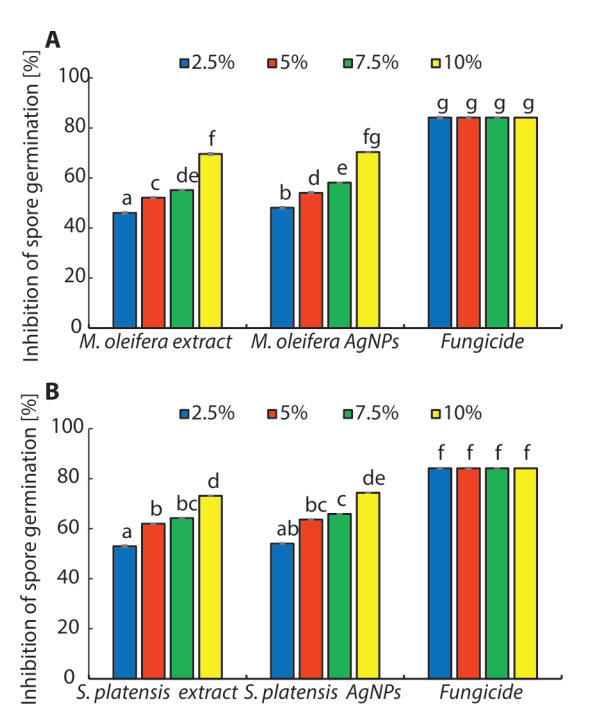


Fig. 10. Inhibition percentage of spore germination of *Aspergillus parasiticus* by crude extract, AgNPs, and fungicide at different concentrations: A – *Morgina oleifera* leaf; B – *Spirulina platensis*. Duncan's multiple range test indicates that there is no significant difference between the lettered columns (p < 0.05, n = 3). The error bars show the SE of the mean

diameters (Fig. 11B). Subsequent treatment with AgNPs from *S. platensis* resulted in severe damage to the hyphae, causing them to flatten, collapse, and appear empty with longitudinal folds (Fig. 11C).

TEM observations

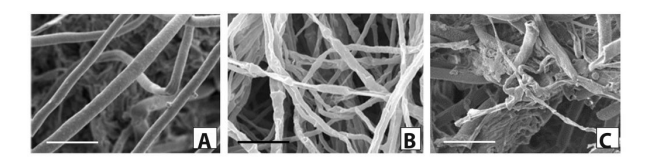
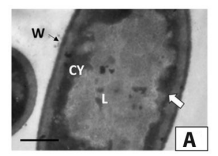


Fig. 11. SEM micrographs of *Aspergillus parasiticus* mycelium grown on PDA after 7 days of incubation at 28°C. A – control (untreated); B – treated hyphae with 10% AgNPs biosynthesized from *Morgina oleifera* leaf extract; C – treated hyphae with 10% AgNPs biosynthesized from *Spirulina platensis* extract. Scale Bar of all micrographs = 20 µm

TEM observations were conducted to further investigate changes in the hyphal structure of A. parasiticus when treated with the highest concentration of 10% AgNPs biosynthesized from M. oleifera leaf and S. platensis extracts. In the control culture that was 7 days old, the hyphal cell's wall and plasma membrane appeared to have unfolded and remained unchanged throughout all parts. The cell cytoplasm appeared normal and uniform, containing large lipid droplets (Fig. 12A). However, in the culture treated with 10% AgNPs biosynthesized from M. oleifera leaf extract, significant devastation and lysis of hyphae were observed. Additionally, there were membranous organelles present and a substantial vacuolation of cytoplasm (Fig. 12B). As for the hyphae treated with 10% AgNPs of S. platensis extract, extreme vacuolation of the hyphae was observed, and the cell organelles were completely unrecognizable and autolyzed (Fig. 12C).





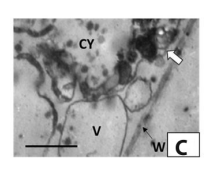


Fig. 12. TEM micrographs of hyphae of *Aspergillus parasiticus* grown on PDA medium after incubation at 28°C. A – control (untreated) showing normal hyphal cells with an intact cell wall (W), intact plasma membrane (arrow), cytoplasm (CY), and lipid globules (L); B – hyphae treated with 10% AgNPs biosynthesized from *Morgina oleifera* leaf extract show the damaged wall (W), disintegrated cytoplasm (CY), damaged plasma membrane (arrow), and large vacuoles (V); C – hyphae treated with AgNPs biosynthesized from *Spirulina platensis* extract. Note the affected wall (W), highly disintegrated cytoplasm (CY), and large vacuoles (V). Note also that the plasma membrane (arrow) is away from the wall. Scale Bars for all micrographs are 1.0 μm

Discussion

The current research aimed to assess the impact of AgNPs biosynthesized from extracts of M. oleifera leaf and S. platensis on the growth and ultrastructure of the aflatoxigenic fungus A. parasiticus, which was isolated from Egyptian wheat grains. Due to the challenges associated with traditional methods for detecting aflatoxin-producing Aspergillus, scientists have shifted towards new and more sensitive techniques for early identification of food contamination by various aflatoxigenic Aspergillus species (Bintvihok et al. 2016). In the current study, 10 A. parasiticus isolates consistently showed aflatoxin production, as confirmed by HPLC, with AFB1 being produced in higher quantities than AFB2. Nevertheless, there was full agreement between the outcomes of these tests on the aflatoxin-producing isolates in the presence of candidate genes and those obtained through other standard methods (Rahimi et al. 2016).

Numerous factors can influence the production of aflatoxins. Temperature, water activity, oxidative stress, and other abiotic variables all play a role in the ability of *A. parasiticus* to produce aflatoxin. These factors are likely to affect different metabolic processes and modify the production of aflatoxin. The presence of aflatoxin was observed at 28°C in liquid medium and 37°C in solid medium (Wanga *et al.* 2019).

The principal aim of this investigation was to ascertain an eco-friendly approach to restrict the proliferation of these troublesome fungi, given that isolated aflatoxigenic fungi generate higher quantities of aflatoxins than previously estimated. Extensive research carried out in recent decades has substantiated the efficacy of diverse plant and microalgae extracts as antifungal agents in inhibiting the growth of aflatoxin-producing fungi and curtailing the synthesis of their toxins (Al-Ghanayem 2017; de Almeida *et al.* 2021; Schoss *et al.* 2022; Ilyas and Manohara 2023).

Antifungal properties of water-based extracts from *M. oleifera* leaf and *S. platensis* were investigated in this research, specifically against aflatoxigenic isolates of *A. parasiticus*, focusing on inhibiting linear mycelial growth and spore germination. The effectiveness of the two extracts varied, with the extract of *S. platensis* displaying the strongest antifungal activity, followed by the extract from *M. oleifera* leaves. This discrepancy can be attributed to more total phenolic compounds found in the *S. platensis* extract, as indicated by HPLC analysis.

Phenolic compounds possess bioactive structures, making them highly valuable as antioxidants and scavengers of free radicals in plants. By donating hydrogen atoms they effectively disrupt chain reactions initiated by free radicals (Torres *et al.* 2018; Baka and El-Zahed



2023). These phenolic chemicals interact with various free radicals, resulting in antioxidant effects. Numerous studies (Sallam *et al.* 2021; Tang *et al.* 2021; Akbari *et al.* 2022; Sindhu *et al.* 2022; Baka and El-Zahed 2023) have demonstrated that hydrogen atom transfer, single electron transfer, sequential proton loss, electron transfer, or transition metal chelation are the mechanisms behind these antioxidant effects.

Chlorogenic acid and epicatechin were found to be the predominant phenolic compounds in *M. oleifera* and *S. platensis*, respectively. According to Khalid *et al.* (2023), the methanolic extract of *M. oleifera* leaf is rich in phenolic compounds, including phenolic acids and flavonoids, and has potential antibacterial properties. Hidayati *et al.* (2020) reported that *S. platensis* is a more valuable source of phenolic compounds than other plant tissues mentioned in the literature. The aqueous extract of *S. platensis* also demonstrated inhibitory effects on the growth of *A. parasiticus*, as observed in studies by Al-Ghanayem (2017) and Abdel-Moneim *et al.* (2022). Antifungal activity of the *S. platensis* extract may be attributed to its intracellular and extracellular metabolites (Al-Ghanayem 2017).

Based on the findings of Martínez et al. (2017), chlorogenic acid (CGA) plays a significant role in enhancing the resistance of various plant species against pathogen attacks. When CGA is converted into chlorogenoquinone, it interacts with free amino acids and proteins, reducing the bioavailability of amino acids, making it harder to digest dietary proteins. In laboratory settings, chlorogenic acid demonstrates a wideranging antifungal effect, effectively preventing spore germination or inhibiting hyphal growth. Unlike fungistatic chemicals, CGA also acts as a fungicide. According to Llorent-Martínez et al. (2017), CGA causes fungal spore membranes to permeabilize quickly, which could lead to a decrease in vitality. Additionally, Rhimi et al. (2020) suggest that chlorogenic acid can act as an antifungal agent by modifying the cell membrane structure of Candida albicans. These studies highlight chlorogenic acid as a promising candidate for developing bioactive alternatives to treat fungal infections.

Epicatechin, a natural flavonoid polyphenol antioxidant found in various plants, belongs to the catechin antioxidant family, alongside other polyphenols like epigallocatechin gallate (Bernatoniene and Kopustinskiene 2018). Hervay *et al.* (2023) highlighted antifungal properties of catechin and epicatechin. Molina-Hernández *et al.* (2022) reported that the combination of AgNPs and catechin inhibited the growth and metabolism of *Aspergillus niger* isolated from coffee seeds. The current research has elucidated that the epicatechin derived from *S. platensis* extract can function as an inhibitor of the wall formation of *A. parasiticus*.

Silver nanoparticles (AgNPs) are one of the most commonly utilized nanomaterials in various areas, particularly within the agriculture sector. Plants are the fundamental component of the environment and the primary essential source of nourishment for mankind; hence, understanding the impacts of AgNPs on plant development and improvement is vital for the assessment of potential natural dangers to food security caused by AgNPs (Yan and Chen 2019). The advancement of strategies for environmentally secure "green synthesis" of silver nanoparticles would increase safer production and biological applications of nanosilver (Moga et al. 2023). Many studies on the phytotoxicity effects of silver nanoparticles (AgNPs) have found a strong link between the amount of AgNPs present during exposure and their phytotoxicity. AgNPs can further endanger human health by encroaching on plant life, accumulating there, and eventually making their way into the human body through the food chain. In fact, it has been demonstrated that AgNPs may cycle through several trophic degrees in the terrestrial and aquatic food chains within the ecosystem (Tangaa et al. 2016).

Metallic nanoparticles (NPs) possess unique properties and exhibit characteristic absorption peaks due to their surface plasmon nature (Khan *et al.* 2019). To confirm the formation of AgNPs in the reaction medium, UV-Vis spectroscopy was employed immediately after synthesis. The UV-Vis spectra of artificially generated AgNPs in an aqueous colloidal solution revealed their maximum absorption at 412.94 nm and 423.50 nm for *M. oleifera* leaves and *S. platensis*, respectively, after 72 h. These absorption peaks align with the anticipated surface plasmon behavior of AgNPs (Usha *et al.* 2017).

FTIR analysis was utilized to distinguish the various functional groups of biomolecules in *M. oleifera* leaf and *S. platensis* extracts, which acted as reducing and stabilizing agents for nanoparticles by creating a protective layer on their surfaces (Baka and El-Zahed 2022). The presence of active phytochemicals in the extracts led to the suggestion from FTIR spectra that the synthetic AgNPs were attached to them. This protective layer played a crucial role in stabilizing the nanoparticles and inhibiting their aggregation and agglomeration (Kumar and Dixit 2017).

The biosynthesized AgNPs' crystalline characteristics were investigated using XRD analysis. The XRD pattern revealed the presence of four distinct diffraction peaks for M. oleifera and S. platensis at two theta (θ) angles. These findings confirmed that the biosynthesized AgNPs possess a face-centered cubic (fcc) structure, which is consistent with the report by the Joint Committee on Powder Diffraction Standards (JCPDS), file no. 04-0783 (Al Aboody 2019). Previous research has also documented the bioformulation of fcc-structured crystalline AgNPs derived from various biological sources, such as leaf extracts from

M. oleifera (Mahmood and Hawar 2022), Euphrasia officinalis (Singh et al. 2018), Mangifera indica (Panwar et al. 2022), and S. platensis (Sidorowicz et al. 2022).

In the present study, the TEM images revealed a uniform dispersion of AgNPs, exhibiting a predominantly spherical morphology. Furthermore, the impact of AgNPs derived from M. oleifera leaves and S. platensis on the size distribution and zeta potential measurements of biosynthesized AgNPs was investigated. The z-mean value of the particle size distribution was found to be consistent with the TEM results. Conversely, the mean zeta potential value, which reflects the surface charge of AgNPs in a colloidal solution, was utilized. The presence of high negative or positive potential values in the colloidal solution leads to the formation of colloidal NPs with remarkable physical stability, owing to the electrostatic attraction between individual particles in the solution (Khatami et al. 2015). The evidence of the monodisperse nature of colloidal nanosuspension is further supported by z-values exceeding -30 mV, whereas lower potentials below -5 mV suggest the presence of aggregation and agglomeration (Gumustas et al. 2017).

In contrast to the M. oleifera leaf extract, the biosynthesis of AgNPs from S. platensis extract effectively inhibits fungal growth and spore germination, as indicated by the findings of the present investigation. This disparity could be attributed to the variety of bioagents that are accessible. Furthermore, the AgNPs derived from M. oleifera leaves and S. platensis extracts were employed for the treatment of A. parasiticus hyphae. The outcomes effectively displayed the evident disparity between the treated and untreated mycelia. Notably, the hyphae treated with AgNPs at a concentration of 10% displayed noteworthy alterations when compared to the control group, as observed through SEM analysis. The treated hyphae cells exhibited a notable disintegration of the cell membrane and cell wall, along with cytoplasmic breakdown, as evidenced by TEM imaging. These findings align with the observations made by Al-Otibi et al. (2022) regarding the alteration of the ultrastructure in Bipolaris sp. after AgNPs treatment. Similarly, Hashem et al. (2022) reported similar outcomes for A. terreus and A. flavus when exposed to AgNPs. The current study demonstrated the efficacy of AgNPs as fungicides against A. parasiticus, highlighting the numerous advantages they possess over traditional chemical fungicides. El-Batal et al. (2014) showed that AgNPs hinder ion efflux-containing transit systems. Disruption of ion efflux leads to the accumulation of silver ions, which, at lower concentrations, impedes cellular processes such as respiration and metabolism by releasing molecules. Moreover, Ag++ has a unique ability to combine with oxygen species that are detrimental to cells, causing damage to lipids, proteins, and nucleic acids.

Several constraints, such as fragment size and concentration, affect the efficacy of fungicidal activity. Research has demonstrated that small particles measuring 12.7 nm are highly effective in inhibiting fungal growth. Various studies suggest that AgNPs can adhere to cell membrane surfaces, disrupting permeability and respiratory functions. It is believed that Ag-NPs can penetrate microorganisms and interact with membrane surfaces (Chaturvedi and Verma 2015). The release of silver anions with an electric charge controls pathogen proliferation, while silver itself hinders pathogen metabolism (Banerjee et al. 2014). Lara et al. (2015) observed through TEM analysis that nanosilver interacts with Candida albicans cell membranes, causing structural abnormalities and ultimately cell death. Dragoni-Rosado et al. (2022) observed that AgNPs adversely affected the growth of Colletotrichum spp. and Nigrospora sp. in vitro. The molecular mechanism of AgNPs involves the generation of free radicals, which induce oxidative stress and cell death in most microorganisms by targeting the organelles within bacterial cells (Dakal et al. 2016).

Conclusions

In closing, the aflatoxigenic fungus A. parasiticus, found in Egyptian wheat grains, has been identified both morphologically and molecularly. A. parasiticus isolates demonstrated a higher production of AFB1 than AFB2, as verified through HPLC analysis. The S. platensis extract contained a greater number of phenolic compounds than the M. oleifera leaf extract. Chlorogenic acid and epicatechin were found in the highest concentrations in the M. oleifera leaf and S. platensis extracts, respectively. The growth of fungal mycelium and spore germination were effectively inhibited by the crude extract of bioagents (M. oleifera and S. platensis) as well as their biosynthesized AgNPs. Fungal mycelia treated with crude extracts and AgNPs at a 10% concentration exhibited significant deformation, as observed through SEM and TEM, in comparison to the control.

References

Abdalla A., Stellmacher T., Becker M. 2023. Trends and prospects of change in wheat self-sufficiency in Egypt. Agriculture 13 (7): 1–12. DOI: https://doi.org/10.3390/agriculture13010007

Abdelaziz A.M., Dacrory S., Hashem A.H., Attia M.S., Hasanin M., Fouda H.M., Kamel S., ElSaied H. 2021. Protective role of zinc oxide nanoparticles-based hydrogel against wilt disease of pepper plant. Biocatalysis and Agricultural Biotechnology 35: 102083. DOI: https://doi.org/10.1016/j.bcab.2021.102083



- Abdel-Moneim A.E., El-Saadony M.T., Shehatan A.M., Saad A.M., Aldhumri S.A., Ouda S.M., Mesalam N.M. 2022. Antioxidant and antimicrobial activities of *Spirulina platensis* extracts and biogenic selenium nanoparticles against selected pathogenic bacteria and fungi. Saudi Journal of Biological Sciences 29 (2): 1197–1209. DOI: https://doi.org/10.1016/j.sjbs.2021.09.046
- Akbari B., Baghaei-Yazdi N., Bahmaie M., Abhari F.M. 2022. The role of plant-derived natural antioxidants in reduction of oxidative stress. Biofactors 48 (3): 611–633. DOI: https://doi.org/10.1002/biof.1831
- Al Aboody M.S. 2019. Silver/silver chloride (Ag/AgCl) nanoparticles synthesized from Azadirachta indica latex and its antibiofilm activity against fluconazole resistant Candida tropicalis. Artificial Cells Nanomedicine Biotechnology 47: 2107–2113. DOI: http://doi.org/10.1080/21691401.201 9.1620257
- Al-Ghanayem A.A. 2017. Antimicrobial activity of *Spirulina platensis* extracts against certain pathogenic bacteria and fungi. Advances in Bioresearch 8 (6): 96–101. DOI: https://doi.org/10.15515/abr.0976-4585.8.6.96101
- Al-Otibi F., Alfuzan S.A., Alharbi R.I., Al-Askar A.A., Al-Otaibi R.M., Al Subaie H.F., Moubayed N.M. 2022. Comparative study of antifungal activity of two preparations of green silver nanoparticles from *Portulaca oleracea* extract. Saudi Journal of Biological Sciences 29: 2772–2781. DOI: https://doi.org/10.1016/j.sjbs.2021.12.056
- Badmus J., Oyemomi S., Adedosu O., Yekeen T., Azeez M., Adebayo E., Lateef A., Badeggi U., Botha S., Hussein A. 2020. Photo-assisted bio-fabrication of silver nanoparticles using *Annona muricata* leaf extract: Exploring the antioxidant, anti-diabetic, antimicrobial, and cytotoxic activities. Heliyon 6: e05413. DOI: https://doi.org/10.1016/j.heliyon.2020.e05413
- Baka Z.A., El-Zahed M.M. 2022. Antifungal activity of silver/silicon dioxide nanocomposite on the response of faba bean plants (*Vicia faba* L.) infected by *Botrytis cinerea*. Bioresources and Bioprocessing 9 (102): 1–19. DOI: https://doi.org/10.1186/s40643-022-00591-7
- Baka Z.A.M., El-Zahed M.M. 2023. Phenolic acids and defenserelated enzymes in host-pathogen interaction in *Senecio aegyptius* and the rust fungus, *Puccinia lagenophorae*. Archives of Phytopathology and Plant Protection 56: 721–752. DOI: https://doi.org/10.1080/03235408.2023.2216368
- Banerjee P., Satapathy M., Mukhopahayay A., Das P. 2014. Leaf extract mediated green synthesis of silver nanoparticles from widely available Indian plants: synthesis, characterization, antimicrobial property and toxicity analysis. Bioresources Bioprocessing 1 (3): 1–10. DOI: https://doi.org/10.1186/s40643-014-0003-y
- Bernatoniene J., Kopustinskiene D.M. 2018. The role of catechins in cellular responses to oxidative stress. Molecules 23 (4): 965. DOI: https://doi.org/10.3390/molecules23040965
- Bessey E.A. 2020. Morphology and Taxonomy of Fungi. Alpha Publishing, Delaware, USA, 806 pp.
- Bintvihok A., Treebonmuang S., Srisakwattana K., Nuanchun W., Patthanachai K., Usawang S. 2016. A rapid and sensitive detection of aflatoxin-producing fungus using an optimized polymerase chain reaction (PCR). Toxicology Research 32: 81–87. DOI: https://doi.org/10.5487/TR.2016.32.1.081
- Chaturvedi V., Verma P. 2015. Fabrication of silver nanoparticles from leaf extract of *Butea monosperma* (Flame of Forest) and their inhibitory effect on bloom-forming cyanobacteria. Bioresources and Bioprocessing 2 (18): 1–8. DOI: https://doi.org/10.1186/s40643-015-0048-6
- Dakal T.C., Kumar A., Majumdar R.S., Yadav V. 2016. Mechanistic basis of antimicrobial actions of silver nanoparticles. Frontiers in Microbiology 7 (1831): 1–17. DOI: https://doi.org/10.3389/fmicb.2016.01831
- de Almeida A.R., da Silva I.C., de Souza C.A.P., Avelino J.R.L., Santos J.E.C.C., de Medeiros E.V., Pinto K. M.S. 2021. Plant

- extract as a strategy for the management of seed pathogens: a critical review. Research, Society and Development 10 (14): e174101421846. DOI: http://doi.org/10.33448/rsd-v10i14.21846
- Dhakad A.K., Ikram M., Sharma S., Khan S., Pandey V.V., Singh A. 2019. Biological, nutritional, and therapeutic significance of *Moringa oleifera* Lam. Phytotherapy Research 33 (11): 2870–2903. DOI: https://doi.org/10.1002/ptr.6475
- Dragoni-Rosado, J.1., González-Mederos A.1., Sambolín-Pérez C. 2022. Effect of silver nanoparticles on the growth of *Colletotrichum* spp. and *Nigrospora* sp. Fungal Biotechnology 2 (1): 1–9. DOI: https://doi.org/10.5943/FunBiotec/2/1/1
- El-Batal A.I., El-Sayed M.H., Refaat B.M., Askar A.A. 2014. Marine *Streptomyces cyaneus* strain alex-sk121 mediated eco-friendly synthesis of silver nanoparticles using gamma radiation. Journal of Pharmaceutical Research International 4 (21): 2525–2547. DOI: https://doi.org/10.9734/BJPR/2014/12224
- Gao J., Yang M. J., Xie Z., Lu B.H., Hsiang, T., Liu L.P. 2021. Morphological and molecular identification and pathogenicity of *Alternaria* spp. associated with ginseng in Jilin province, China. Canadian Journal of Plant Pathology 43 (4): 537–550. DOI: https://doi.org/10.1080/07060661.20 20.1858167
- Górniak I., Bartoszewski R., Króliczewski J. 2019. Comprehensive review of antimicrobial activities of plant flavonoids. Phytochemical Review 18: 241–272. DOI: https://doi.org/10.1007/s11101-018-9591-z
- Gumustas M., Sengel-Turk C.T, Gumustas A., Ozkan S.A, Uslu B. 2017. Effect of polymer-based nanoparticles on the assay of antimicrobial drug delivery systems. p. 67–108. In: "Multifunctional Systems for Combined Delivery, Biosensing and Diagnostics" (A.M. Grumezescu, ed.). Elsevier, Amsterdam, The Netherlands, 356 pp.
- Guzmán C., Ibba M.I., Álvarez J.B., Sissons M., Morris C. 2022. Wheat quality. p. 177–193. In: "Wheat Improvement: Food Security in a Changing Climate" (M.P. Reynolds, H.J. Braun, eds.). Springer, Cham, 629 pp. DOI: https://doi.org/10.1007/978-3-030-90673-3_11
- Hasanin M., Elbahnasawy M.A., Shehabeldine A.M., Hashem A.H. 2021. Ecofriendly preparation of silver nanoparticles-based nanocomposite stabilized by polysaccharides with antibacterial, antifungal and antiviral activities. Biometals 34 (6): 1313–1328. DOI: https://doi.org/10.1007/ s10534-021-00344-7
- Hashem A.H., Saied E., Amin B.H., Alotibi F.O., Al-Askar A.A., Arishi A.A., Elkady F.M., Elbahnasawy M.A. 2022. Antifungal activity of biosynthesized silver nanoparticles (AgNPs) against Aspergilli causing Aspergillosis: Ultrastructure study. Journal of Functional Biomaterials 13 (242): 1–17. DOI: https://doi.org/10.3390/jfb13040242
- Hendricks K.E., Christman M.C., Roberts P.D. 2017. A statistical evaluation of methods of in vitro growth assessment for *Phyllosticta citricarpa*: Average colony diameter vs. area. PLoS One 12 (1): e0170755. DOI: https://doi.org/10.1371/journal.pone.0170755
- Hervay N.T., Elias D., Habova M., Jacko J., Morvova Jr. M., Gbelska Y. 2023. Catechin potentiates antifungal effect of miconazole in *Candida glabrata*. Folia Microbiologica 68: 835–842. DOI: https://doi.org/10.1007/s12223-023-01061-z
- Hidayati J.R., Yudiati E., Pringgenies D., Oktaviyanti D.T., Alief Putri Kusuma A.P. 2020. Comparative study on antioxidant activities, total phenolic compound and pigment contents of tropical Spirulina platensis, *Gracilaria arcuata* and *Ulva lactuca* extracted in different solvents polarity. E3S Web of Conferences 147: 03012. DOI: https://doi.org/10.1051/e3sconf/202014703012
- Igrejas G., Branlard G. 2020. The importance of wheat. p. 1–7.
 In: "Wheat Quality For Improving Processing And Human Health" (G. Igrejas, T. Ikeda, C. Guzmán, eds.). Springer, Cham, 554 pp. DOI: https://doi.org/10.1007/978-3-030-34163-3_1

337

www.journals.pan.pl



- Ilyas S., Manohara D. 2023. Seed-borne mycoflora and their management. p. 29–46. In: "Plant Mycobiome: Diversity, Interactions and Uses" (Y.M. Rashad, Z.A.M. Baka, T.A.A. Moussa, eds.) Springer, Cham, 496 pp. DOI: https://doi. org/10.1007/978-3-031-28307-9_2
- Ismail M. A., Abdel-Hafez S.I.I., Hussein N.A., Abdel-Hameed N.A. 2015. Contributions to the Genus *Fusarium* in Egypt with Dichotomous Keys for Identification of Species. Tomasz M. Karpiński ul. Szkółkarska 88B, 62-002 Suchy Las, Poland, 175 pp.
- Jain N. 2023. Spirulina: The future food. Modern Concepts and Developments in Agronomy 12 (3): 1190–1191. DOI: https: //doi.org/10.31031/MCDA.2023.12.000787
- Khalid S., Arshad M., Mahmood S., Ahmed W., Siddique F., Khalid W., Zarlasht M., Asar T.O., Hassan F.A.M. 2023. Nutritional and phytochemical screening of *Moringa oleifera* leaf powder in aqueous and ethanol extract. International Journal of Food Properties 26 (1): 2338–2348. DOI: https:// doi.org/10.1080/10942912.2023.2246685
- Khalil Y.M.M., Abd El-Ghani S.S., Mansour T.G.I. 2020. A standard analysis of Egyptian foreign trade structure for wheat. Bulletin of the National Research Centre 44 (20): 1–7. DOI: https://doi.org/10.1186/s42269-020-0273-9
- Khan I., Saeed K., Khan I. 2019. Nanoparticles: Properties, applications and toxicities. Arabian Journal of Chemistry 12 (7): 908–931. DOI: https://doi.org/10.1016/j.arabjc.2017.05.011
- Khan M.A., Hafeez M., Zaheer M. Hameed U. 2022. Microscopic and biochemical identification of *Spirulina* spp. for its biomass cultivation by using different types of photobioreactors at lab and pilot scale. Pakistan Journal of Biochemistry and Biotechnology 3 (2): 123–131. DOI: https://doi.org/10.52700/pjbb.v3i2.194
- Khatami M., Pourseyedi S., Khatami M., Hamidi H., Mehrnaz Zaeifi M., Soltani L. 2015. Synthesis of silver nanoparticles using seed exudates of *Sinapis arvensis* as a novel bioresource, and evaluation of their antifungal activity. Bioresources and Bioprocessing 2 (19): 1–7. DOI: https://doi.org/10.1186/s40643-015-0043-y
- Kimanya M.E., Routledge M.N., Mpolya E., Ezekiel C.N., Shirima C.P., Gong Y.Y. 2021. Estimating the risk of aflatoxin-induced liver cancer in Tanzania based on biomarker data. PLoS ONE 16 (3): e0247281. DOI: https://doi.org/10.1371/journal.pone.0247281
- Kumar A., Dixit C.K. 2017. Methods for characterization of nanoparticles. p. 43–59. In: "Advances in Nanomedicine for the Delivery of Therapeutic Nucleic Acids" (S. Nimesh, R. Chandra, N. Gupta, eds.), Elsevier: Amsterdam, The Netherlands, 256 pp.
- Lara H.H., Romero-Urbina D.G., Pierce C., Lopez-Ribot J.L., Arellano-Jiménez M.J., Jose-Yacaman M. 2015. Effect of silver nanoparticles on *Candida albicans* biofilms: an ultrastructural study. Journal of Nanobiotechnology 13 (91): 1–12. DOI: https://doi.org/10.1186/s12951-015-0147-8
- Llorent-Martínez E.J, Ortega-Barrales P., Zengin G., Mocan A., Simirgiotis M.J., Ceylan R., Uysal S., Aktumsek A. 2017. Evaluation of antioxidant potential, enzyme inhibition activity and phenolic profile of *Lathyrus cicera* and *Lathyrus digitatus*: Potential sources of bioactive compounds for the food industry. Food and Chemical Toxicology 107 (Pt B): 609–619. DOI: https://doi.org/10.1016/j.fct.2017.03.002
- Lobiuc A., Paval N.E., Mangalagiu I.I., Gheorghita R., Teliban G.C., Amariucai-Mantu D., Stoleru V. 2023. Future antimicrobials: Natural and Functionalized Phenolics. Molecules 28 (1114): 1–16. DOI: https://doi.org/10.3390/molecules28031114
- Mahmood G., Hawar S.N. 2022. Green biosynthesis of silver nanoparticles from *Moringa oleifera* leaves and its antimicrobial and cytotoxicity activities. International Journal of Biomaterials 2022: 1–10. DOI: https://doi.org/10.1155/2022/4136641
- Martínez G., Regente M., Jacobi S., Del Rio M., Pinedo M., Laura de la Canal L. 2017. Chlorogenic acid is a fungicide ac-

- tive against phytopathogenic fungi. Pesticide Biochemistry and Physiology 140: 30–35. DOI: https://doi.org/10.1016/j.pestbp.2017.05.012
- Medda S., Hajra A., Dey U., Bose P., Mondal N.K. 2015. Biosynthesis of silver nanoparticles from *Aloe vera* leaf extract and antifungal activity against *Rhizopus* sp. and *Aspergillus* sp. Applied Nanoscience 5: 875–880. DOI: https://doi.org/10.1007/s13204-014-0387-1
- Molina-Hernández J.B., Scroccarello A., Pelle F.D., De Flaviis R., Compagnone D., Del Carlo M., Paparella A., Clemencia Chaves López C.C. 2022. Synergistic antifungal activity of catechin and silver nanoparticles on *Aspergillus niger* isolated from coffee seeds. LWT 169: 113990. DOI: https://doi.org/10.1016/j.lwt.2022.113990
- Neves A.C., Viana A.D., Menezes F.G., Neto A.O.W., Melo M.C.N., Gasparotto L.H. 2021. Biospectroscopy and chemometrics as an analytical tool for comparing the antibacterial mechanism of silver nanoparticles with popular antibiotics against *Escherichia coli*. Spectrochimica Acta Part A: Molecular and Biomolecular Spectroscopy 253: 119558. DOI: https://doi.org/10.1016/j.saa.2021.119558
- Nyongesa B.W., Okoth S., Ayugi V. 2015. Identification Key for *Aspergillus* species isolated from maize and soil of Nandi County, Kenya. Advances in Microbiology 5: 205–229. DOI: https://doi.org/10.4236/aim.2015.54020
- Pagnussatt F.A., de Lima V.R., Dora C.L., Costa J.A.V., PutauxJ-L., Badiale-Furlong E. 2016. Assessment of the encapsulation effect of phenolic compounds from *Spirulina* sp. LEB-18 on their antifusarium activities. Food Chemistry 211: 616–623. DOI: https://doi.org/10.1016/j.foodchem.2016.05.098
- Panwar R.S., Pervaiz N., Dhillon G., Kumar S., Sharma N., Aggarwal N., Tripathi S., Kumar R., Vashisht A., Kumar N. 2022. *Mangifera indica* leaf extract assisted biogenic silver nanoparticles potentiates photocatalytic activity and cytotoxicity. Journal of Materials Science: Materials in Electronics 33 (2):1-12. DOI: https://doi.org/10.1007/s10854-022-08546-6.
- Patil S.V., Mohite B.V., Marathe K.R., Salunkhe N.S., Marathe V., Patil V.S. 2022. *Moringa* tree, gift of nature: a review on nutritional and industrial potential. Current Pharmacological Reports 8: 262–280. DOI: https://doi.org/10.1007/s40495-022-00288-7
- Rahimi S., Sohrabi N., Ebrahimi M.A., Tebyanian M., Taghizadeh M., Rahimi S. 2016. Application of PCR in the detection of aflatoxinogenic and non-aflatoxinogenic strains of *Aspergillus parasiticus* group of cattle feed isolated in Iran. Journal of Molecular Biology Research 6 (1): 121–128. DOI: https://doi.org/10.5539/jmbr.v6n1p121
- Rhimi W., Aneke C.I., Annoscia G., Otranto D., Boekhout T., Claudia Cafarchia C. 2020. Effect of chlorogenic and gallic acids combined with azoles on antifungal susceptibility and virulence of multidrug-resistant Candida spp. and Malassezia furfur isolates. Medical Mycology 58 (8): 1091–1101. DOI: https://doi.org/10.1093/mmy/myaa010
- Salem S.S., Ali O.M., Reyad A.M., Abd-Elsalam K.A., Amr H., Hashem A.H. 2022. *Pseudomonas indica*-mediated silver nanoparticles: Antifungal and antioxidant biogenic tool for suppressing mucormycosis fungi. Journal of Fungi 8 (126): 1–13. DOI: https://doi.org/10.3390/jof8020126
- Sallam N.M.A., Ali E.F., Abo-Elyousr K.A.M., Bereika M.F.F., Seleim M.A.A. 2021. Thyme oil treatment controls bacterial wilt disease symptoms by inducing antioxidant enzyme activity in *Solanum tuberosum*. Journal of Plant Pathology 103 (2): 563–572. DOI: https://doi.org/10.1007/s42161-021-00808-2
- Salleh A., Naomi R., Utami N.D., Mohammad A.W., Mahmoudi E., Mustafa N., Fauzi M.B. 2020. The potential of silver nanoparticles for antiviral and antibacterial applications: A mechanism of action. Nanomaterials 10 (8): 1566. DOI: https://doi.org/10.3390/nano10081566



- Shabeer S., Asad S., Jamal A., Ali A. 2022. Aflatoxin contamination, its impact and management strategies: An updated review. Toxins 14 (5): 307. DOI: https://doi.org/10.3390/toxins14050307
- Schmidt M., Horstmann S., De Colli L., Danaher M., Speer K., Zannini E., Arendt E.K. 2016. Impact of fungal contamination of wheat on grain quality criteria. Journal of Cereal Science 69: 95–103. DOI: https://doi.org/10.1016/j.jcs.2016.02.010
- Schoss K., Glavac N.K., Koce J.D., Anžlovar S. 2022. Supercritical CO₂ plant extracts show antifungal activities against crop-borne fungi. Molecules 27 (3): 1132. DOI: https://doi. org/10.3390/molecules27031132
- Shishido T.K., Humisto A., Jokela J., Liwei Liu L., Wahlsten M., Tamrakar A., Fewer D.P., Permi P., Andreote A.P.D., Fiore M.F., Kaarina Sivonen K. 2015. Antifungal compounds from cyanobacteria. Marine Drugs 13 (4): 2124–2140. DOI: https://doi.org/10.3390/md13042124
- Sidorowicz A., Margarita V., Fais G., Pantaleo A., Manca A., Concas A., Rappelli P., Fiori P.L., Giacomo C. 2022. Characterization of nanomaterials synthesized from *Spirulina platensis* extract and their potential antifungal activity. PloS ONE 17 (9): e0274753. DOI: https://doi/org/10.1371/journal.pone.0274753
- Sindhu R.K., Kaur P., Kaur P., Singh H., Batiha G.E., Verma I. 2022. Exploring multifunctional antioxidants as potential agents for management of neurological disorders. Environmental Science of Pollution Research International 29 (17): 24458–24477. DOI: https://doi.org/10.1007/s11356-021-17667-0
- Singh H., Du J., Singh P., Yi T.H. 2018. Ecofriendly synthesis of silver and gold nanoparticles by *Euphrasia officinalis* leaf extract and its biomedical applications. Artificial Cells Nanomedicine and Biotechnology 46 (6): 1163–1170. DOI: https://doi.org/10.1080/21691401.2017.1362417
- Soni R.A., Sudhakar K., Rana S.R.S. 2019. Comparative study on the growth performance of *Spirulina platensis* on modifying culture media. Energy Reports 5: 327–336. DOI: https://doi. org/10.1016/j.egyr.2019.02.009
- Tang G., Xu Y., Zhang C., Wang N., Li H., Feng Y. 2021. Green tea and epigallocatechin gallate (EGCG) for the management of nonalcoholic fatty liver diseases (NAFLD): Insights into the role of oxidative stress and antioxidant mechanism.

- Antioxidants 10 (7): 1076. DOI: https://doi.org/10.3390/antiox10071076
- Tangaa S.R., Selck H., Winther-Nielsen M., Khan F.R. 2016. Trophic transfer of metal-based nanoparticles in aquatic environments: A review and recommendations for future research focus. Environmental Science Nano 3: 966–981. DOI: https://doi.org/10.1039/C5EN00280J
- Trombete F.M., Santos T.B., Direito G.M., Fraga M.E., Saldanha T. 2014. In-house validation of a method for determining aflatoxins B1, B2, G1 and G2 in wheat and wheat by-products. Pesquisa Agropecuaria Tropical 44: 255–262. DOI: https://doi.org/10.1590/S1983-40632014000300003
- Torres C.A., Zamora C.M.P., Nuñez M.B., Gonzalez A.M. 2018. In vitro antioxidant, antilipoxygenase and antimicrobial activities of extracts from seven climbing plants belonging to the Bignoniaceae. Journal of Integrative Medicine 16: 255–262. DOI: https://doi.org/10.1016/j.joim.2018.04.009
- Usha S., Ramappa K.T., Hiregoudar S., Vasanthkumar G.D., Aswathanarayana D.S. 2017. Biosynthesis and characterization of copper nanoparticles from tulasi (*Ocimum sanctum* L.) leaves. International Journal of Current Microbiology and Applied Sciences 6 (11): 2219–2228. DOI: https://doi. org/10.20546/ijcmas.2017.611.263
- Wanga P., Changb P.K., Konga Q., Shanc S., Weib Q. 2019. Comparison of aflatoxin production of Aspergillus parasiticus at different temperatures and media: Proteome analysis based on TMT. International Journal of Food Microbiology 310: 108313. DOI: https://doi.org/10.1016/j.ijfoodmicro.2019.108313
- Yadav S., Goswami P., Mathur J. 2023. Evaluation of fungicidal efficacy of *Moringa oleifera* Lam. leaf extract against Fusarium wilt in wheat. Journal of Natural Pesticide Research. 4: 100034. DOI: https://doi.org/10.1016/j.napere.2023.100034
- Yan A., Chen Z. 2019. Impacts of silver nanoparticles on plants: A Focus on the Phytotoxicity and underlying mechanism. International Journal of Molecular Sciences 20 (5):1003. DOI: https://doi.org/10.3390/ijms20051003
- Zanganeh E., Mirzaei H., Jafari S.M., Javadi A., Afshar Mogaddam M.R. 2022. *Spirulina platensis* extract nanoliposomes: Preparation, characterization, and application to white cheese. Journal of AOAC International 105: 827–834. DOI: https://doi/org/10.1093/jaoacint/qsab162